

Self propulsion of droplets driven by an active permeating gel

R. Kree and A. Zippelius

Georg-August-Universität Göttingen, Institut für Theoretische Physik,
Friedrich-Hund-Platz 1, 37077 Göttingen, Germany

March 9, 2022

Abstract

We discuss the flow field and propulsion velocity of active droplets, which are driven by body forces residing on a rigid gel. The latter is modelled as a porous medium which gives rise to permeation forces. In the simplest model, the Brinkman equation, the porous medium is characterised by a single length scale ℓ – the square root of the permeability. We compute the flow fields inside and outside of the droplet as well as the energy dissipation as a function of ℓ . We furthermore show that there are optimal gel fractions, giving rise to maximal linear and rotational velocities. In the limit $\ell \rightarrow \infty$, corresponding to a very dilute gel, we recover Stokes flow. The opposite limit, $\ell \rightarrow 0$, corresponding to a space filling gel, is singular and not equivalent to Darcy’s equation, which cannot account for self-propulsion

1 Introduction

Hydrodynamic models of self-propelled particles [1] have focused primarily on either squirmers built on ciliary propulsion or phoretic effects – both localised on the surface of the swimmer. Here we consider instead active forces in the interior of a living organism or cell. The complex spatial organisation of a cell includes a network of filaments, which serves not only as a backbone but also provides the tracks for active transport by motor proteins. Biomolecules, vesicles or even organelles can be actively transported in this way, thereby generating flow in the cytosol. Cytoplasmic streaming has been discussed

extensively [2] in the context of intracellular transport. However sustained flow of the cytosol can have various other effects. Here we discuss the possibility of self-propulsion: Active forces generate internal flow which in turn gives rise to swimming motion [3].

Coarse grained models of the cell interior are frequently based on multi-component or multi-phase systems, in the simplest case a two fluid model [4] or a biphasic system, representing the filamentary network and the interstitial fluid [5]. We built on this work and model the cytoplasm as a biphasic system, consisting of a gel and a sol phase. The gel is modeled as a porous medium and the sol as a Newtonian fluid. Poroelastic materials as a model for the cytoplasm [6] have been discussed i.a. in the context of force-indentation curves of cells. Here, we assume that the active forces are localised on the gel and drive permeation flows in the sol [7]. As a first step, we ignore the elasticity of the porous gel and assume the gel to be rigid. Within this approximation the dynamics of the gel is restricted to rigid body motion and the flow of the fluid component follows Brinkman’s equation. The resulting model can be solved analytically, allowing us to compute the linear and angular velocity of propulsion as well as the flow fields inside and outside of the droplet.

Our study gets further motivation from increasing experimental efforts to construct simplified biomimetic devices or even synthesize artificial cells with controlled ingredients and the ability for self-assembly, active processes and some degree of functionality. Mixtures of actin filaments, cross-linkers and motor proteins exhibit stationary dy-

dynamic states with high activity [8]. Active nematics of microtubules and motors inside lipid vesicles also exhibit dynamic states, sometimes periodic and possibly shape changing [9]. More recently droplet stabilised vesicles [10] have been assembled and loaded with biomolecules to synthesize increasingly more complex, functional cells in aqueous solution. Theoretical approaches have suggested that active droplets may serve as models for protocells [11]. Droplets generated by phase separation provide compartments for the spatial organization of chemicals with their size being controlled by chemical reaction rates [12]. Active droplets were furthermore shown to spontaneously split into two identical daughter cells [11], thus behaving similarly to cells. Here we focus on the active motion of biphasic droplets.

The paper is organized as follows. We introduce the model in sec. 2. Linear and rotational motion of the droplet as well as the interior flow fields are presented in sec. 3 and sec. 4. The singular limit of very small permeation length is discussed in sec. 5, where we also show that Darcy's equation cannot account for self-propulsion. Finally, in sec. 6 we present our conclusions and give an outlook to future work. Details of the calculation are delegated to 3 appendices.

2 Model

We consider a neutrally buoyant spherical droplet of radius $R = 1$, immersed into an incompressible Newtonian fluid of viscosity η^+ . The interior of the droplet is composed of a statistically homogeneous and isotropic rigid gel coexisting with another incompressible fluid of viscosity η . Both the internal fluid and the gel are assumed to be completely immiscible in the ambient fluid. The volume fraction occupied by the gel (gel fraction) will be denoted by ϕ . The disorder or volume averaged flow velocity field \mathbf{v} inside the droplet is assumed to obey the Brinkman equation [13, 14]

$$\nabla^2 \mathbf{v}(\mathbf{r}) - \frac{1}{\kappa(\phi)} (\mathbf{v}(\mathbf{r}) - \mathbf{v}^{gel}) = \frac{1}{\eta} (\nabla p(\mathbf{r}) - \mathbf{f}^{act}(\mathbf{r}, \phi)). \quad (1)$$

Here $\kappa(\phi)$ denotes the intrinsic permeability, which depends on the details of the gel structure, the pres-

sure field $p(\mathbf{r})$ is determined from the incompressibility constraint $\nabla \cdot \mathbf{v} = 0$ and the body force density \mathbf{f}^{act} is due to active processes in the gel, which drive permeation flows. As an example, one may think of cargo particles actively moving on a random network of stiff filaments, thereby generating flow (see sketch in Fig 1). We introduce a frame of reference with its origin at the center of the sphere. In this frame the velocity of the rigid gel must be of the form

$$\mathbf{v}^{gel}(\mathbf{r}) = \mathbf{v}_g + \boldsymbol{\omega}_g \times \mathbf{r} \quad (2)$$

with constant vectors \mathbf{v}_g and $\boldsymbol{\omega}_g$.

All passive properties of the gel, which influence the flow field \mathbf{v} are subsumed in the permeability κ and the viscosity η . In polymeric gels, the length scale $\sqrt{\kappa} = \ell$ is also referred to as the hydrodynamic screening length. There are many models in the literature [15], which relate κ to other macroscopic properties of the gel (for example gel fraction, specific surface area and tortuosity). Here, we restrict our attention to the dependence of κ on the gel fraction ϕ . Without any additional information about the gel structure, we consider $\kappa(\phi)$ as a smooth monotonic function, which varies between the obvious limiting cases (i) $\kappa \rightarrow 0$ for $\phi \rightarrow 1$ and (ii) $\kappa \rightarrow \infty$ if $\phi \rightarrow 0$. κ may vanish before $\phi = 1$ is reached, if the fluid no longer percolates. Here we are not interested in the behaviour close to the percolation threshold and choose a variant of the classical Carman-Kozeny formula [16]

$$\kappa(\phi) = \ell^2 = \ell_0^2 (1 - \phi)^2 / \phi^2 \quad (3)$$

for purposes of illustration. Our qualitative results do not depend on the precise form of $\kappa(\phi)$. As the force density $\mathbf{f}^{act}(\mathbf{r}, \phi)$ is assumed to result from active elements, which are distributed smoothly over the gel, we assume that $\mathbf{f}^{act}(\mathbf{r}, \phi) \propto \phi$.

Outside of the volume V , the flow velocity field \mathbf{v}^+ satisfies Stokes equation without the permeation force and without active forces. Boundary conditions at an interface ∂V between a porous medium and a Newtonian fluid are still discussed in the literature. Various different forms have been proposed [17] [18] [19][20], depending upon the microstructure of the interfaces both between internal and ambient fluid

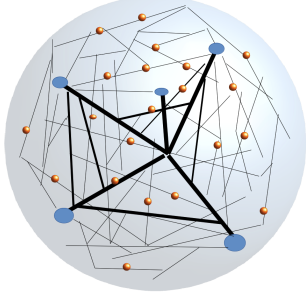


Figure 1: Our model is a continuum version of the sketched situation, where actively transported particles (for example vesicles) move along the rigid filaments of a gel.

and between gel and ambient fluid. Here we consider the simplest situation, which occurs if the gel phase is wetted by a layer of internal fluid, thus avoiding any interface with the ambient fluid. Otherwise, the stresses at the interface would have to be divided into viscous stresses and solid stresses. Furthermore, if a large fraction of the interface is solid, the situation may be complicated by the appearance of velocity slips. For the simple fluid-fluid interface considered here, we can assume that there is no velocity slip, i.e. the tangential velocity component is continuous across the interface. In combination with the condition of immiscibility, this leads to the continuity of \mathbf{v} across ∂V ,

$$\mathbf{v}^+(\mathbf{r}) = \mathbf{v}(\mathbf{r}) \quad \text{for } \mathbf{r} \in \partial V. \quad (4)$$

A second boundary condition at ∂V simply states that the interface is force free:

$$\boldsymbol{\sigma}^+ \cdot \mathbf{e}_r - \boldsymbol{\sigma}^- \cdot \mathbf{e}_r = 2\gamma_0 \mathbf{e}_r. \quad (5)$$

The balance of forces includes the viscous tractions $\mathbf{t}^\pm = \pm \boldsymbol{\sigma}^\pm \cdot \mathbf{e}_r$ with $\sigma_{ij}^- = \sigma_{ij}(\mathbf{v}) = -p\delta_{ij} + \eta(\partial_j v_i + \partial_i v_j)$ and $\sigma_{ij}^+ = \sigma_{ij}(\mathbf{v}^+)$ and the Laplace pressure $2\gamma_0 \mathbf{e}_r$ resulting from a homogeneous surface tension γ_0 .

We are interested in an autonomous swimmer and hence require that it be force and torque free, so that

$\int_V \mathbf{f}^{act} d^3r = 0$ and $\int_V \mathbf{r} \times \mathbf{f}^{act} d^3r = 0$ hold. Integrating the Brinkman equation over the volume (directly and after multiplying by $\mathbf{r} \times$) relates \mathbf{v}_g and $\boldsymbol{\omega}_g$ to the internal flow field:

$$\int_V d^3x \mathbf{v} = \int_V d^3x \mathbf{v}_g = \frac{4\pi}{3} \mathbf{v}_g \quad (6)$$

$$\int_V d^3x \mathbf{r} \times \mathbf{v} = \int_V d^3x \mathbf{r} \times (\boldsymbol{\omega}_g \times \mathbf{r}) = \frac{8\pi}{15} \boldsymbol{\omega}_g \quad (7)$$

Brinkman's equation allows for the same expansion in vector spherical harmonics as Stokes equation, suggesting a representation of the active force densities in the same set of functions. The self-propelling properties of arbitrary force densities and tractions are entirely determined by their $l = 1$ component, so that we restrict the expansion to $l = 1$:

$$\mathbf{f}^{act} = \alpha(r)Y_{10}\mathbf{e}_r + \beta(r)\nabla_s Y_{10} + \gamma(r)\mathbf{e}_r \times \nabla_s Y_{10}. \quad (8)$$

We further simplify the discussion by considering only $m = 0$, which leads to parallel directions of linear and angular velocity. The generalization to $m = \pm 1$ and to $l \geq 1$ is straightforward.

The functions $\alpha(r), \beta(r), \gamma(r)$ are restricted by the requirements of vanishing total force and torque, implying

$$\int_0^1 (\alpha(r) + 2\beta(r))r^2 dr = 0 \quad (9)$$

and

$$\int_0^1 \gamma(r)r^3 dr = 0. \quad (10)$$

3 Linear motion

As for Stokes flow, we can decompose active forces and the resulting flow into a chiral part ($\propto \gamma(r)$), giving rise to rotations of the droplet around the polar axis \mathbf{e}_z of the spherical coordinates, and a non-chiral part, giving rise to linear motion in \mathbf{e}_z direction. In terms of vector spherical harmonics $\mathbf{e}_z = (\sqrt{4\pi/3})(\mathbf{e}_r Y_{10} + \nabla_s Y_{10})$, so that $\mathbf{v}_g = v_g \mathbf{e}_z = v_{g,0} \mathbf{e}_r Y_{10} + v_{g,1} \nabla_s Y_{10}$ with $v_{g,0} = v_{g,1} = \sqrt{4\pi/3} v_g$ (and analogously for $\boldsymbol{\omega}_g$). Note that v_g and $\boldsymbol{\omega}_g$ still have to be determined as part of the solution. We first consider linear motion and hence put $\gamma(r) = 0$; subsequently we are going to discuss the rotational motion with non-vanishing $\gamma(r)$.

3.1 Solution of Brinkman's equation

We use the following ansatz for the solution of Brinkman's equation: $\mathbf{v} - \mathbf{v}_g = \mathbf{v}^{hom} + \mathbf{v}^{inh}$. The first term on the right hand side, \mathbf{v}^{hom} , is the solution of the homogeneous equation

$$\nabla^2 \mathbf{v}^{hom}(\mathbf{r}) - \frac{1}{\kappa(\phi)} \mathbf{v}^{hom} = 0. \quad (11)$$

The second term, \mathbf{v}^{inh} , denotes a special solution of the inhomogeneous equation. Given the restriction to the $l = 1, m = 0$ components of the active forces, we represent \mathbf{v}^{inh} as:

$$\mathbf{v}^{inh} = v_0^{inh}(r) Y_{10}(\theta, \varphi) \mathbf{e}_r + v_1^{inh}(r) \nabla_s Y_{10}(\theta, \varphi). \quad (12)$$

The requirement of incompressibility, which reads explicitly $v_1(r) = (r/2) dv_0(r)/dr + v_0(r)$, can be used to reduce Eq. (11) to a single equation for $v_0^{inh}(r)$:

$$\left(\frac{d^2}{dr^2} + \frac{4}{r} \frac{d}{dr} - \frac{1}{\kappa} \right) v_0^{inh}(r) = 0. \quad (13)$$

This equation has two fundamental solutions, one regular at the origin and one regular for $r \rightarrow \infty$. For the interior of the droplet we pick the one which is regular at the origin, which is $v_0^{inh}(r) = Au_0(r/\sqrt{\kappa})$ with

$$u_0(x) = \frac{1}{x} \left(\frac{\sinh(x)}{x^2} - \frac{\cosh(x)}{x} \right) = x^{-3/2} I_{3/2}(x) \quad (14)$$

Here $I_{3/2}(x)$ denotes a modified Bessel function I_ν as defined in [21].

To solve the inhomogeneous equation, we first determine the pressure, using incompressibility to write $\nabla^2 p = \nabla \cdot \mathbf{f}^{act}$. The general solution (regular at the origin) is given by $p(\mathbf{r}) = (p_0 r + p^{inh}(r)) Y_{10}(\theta, \varphi)$, where $p^{inh}(r)$ has to be determined from

$$\left(\frac{d^2}{dr^2} + \frac{2}{r} \frac{d}{dr} - \frac{2}{r^2} \right) p^{inh} = \frac{d\alpha}{dr} + \frac{2}{r}(\alpha - \beta). \quad (15)$$

The inhomogeneous velocity, \mathbf{v}^{inh} is expanded in analogy to the homogeneous component

$$\mathbf{v}^{inh} = v_0^{inh}(r) Y_{10}(\theta, \varphi) \mathbf{e}_r + v_1^{inh}(r) \nabla_s Y_{10}(\theta, \varphi). \quad (16)$$

and $v_0^{inh}(r)$ is a special solution of the inhomogeneous equation

$$\left(\frac{d^2}{dr^2} + \frac{4}{r} \frac{d}{dr} - \frac{1}{\kappa} \right) v_0^{inh}(r) = \frac{1}{\eta} \left(p_0 + \frac{dp^{inh}}{dr} - \alpha(r) \right). \quad (17)$$

We will consider explicit forms of $\alpha(r)$ and $\beta(r)$ later to illustrate the solution. Note that \mathbf{v}^{inh} depends upon the pressure coefficient p_0 , which has to be determined from boundary conditions. In the following we make this dependence explicit and split $v_0^{inh}(r) = w_0(r) - (\kappa/\eta)p_0$.

The external flow field $v_0^+(r) = a^+/r + b^+/r^3$ is the well known solution of the Stokes problem. Our solution thus contains four constants, A, p_0, a^+, b^+ and the boundary conditions, Eq.(4) and Eq.(5), provide a system of four linear equations to determine them (see Appendix A for further details). The force free condition implies the absence of a Stokeslet, i.e. $a^+ = 0$.

As shown in Appendix A, linear motion leads to the radial flow field $\mathbf{v}_r = \sqrt{3/4\pi} v_0(r) \cos \theta \mathbf{e}_r$ with

$$v_0(r) = A[u_0(r/\sqrt{\kappa}) - u_0(1/\sqrt{\kappa})] + [w_0(r) - w_0(1)] + v_{g,0}. \quad (18)$$

The tangential flow field $\mathbf{v}_t = -\sqrt{3/4\pi} v_1(r) \sin \theta \mathbf{e}_\theta$ is determined from the incompressibility condition. The center of mass velocity turns out to be $v_{g,0} = -(Au'_0(1) + w'_0(1))/3$ and for the constant A we find

$$A = - \left(\frac{2(\eta^+ - \eta)w'_0 + w_0\eta/\kappa + p^{inh}}{2(\eta^+ - \eta)u'_0 + u_0\eta/\kappa} \right)_{r=1}. \quad (19)$$

Here $p^{inh}(r)$ and $w_0(r)$ depend on the active driving forces which have yet to be specified. We first discuss a monotonic force density and subsequently introduce a nonmonotonic force, varying on a length-scale smaller than the size of the droplet.

3.2 Examples of simple force densities

We find analytical solutions for any polynomial force density, as discussed in detail in Appendix B. A particularly simple example is $\alpha(r) = -2\beta(r) = \alpha\phi r^2$, which gives rise to the following inhomogeneous so-

lution:

$$p^{inh}(r) = \frac{\alpha\phi}{2}r^3 \quad (20)$$

$$w_0(r) = -\frac{\alpha\phi\kappa}{2\eta}(r^2 + 10\kappa). \quad (21)$$

The resulting center of mass velocity is shown in

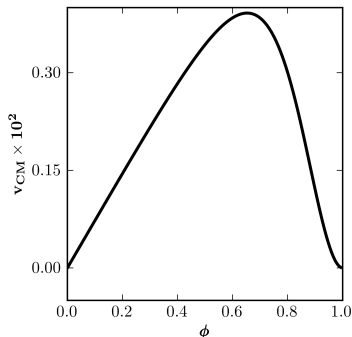


Figure 2: Center of mass velocity of the droplet vs. gel fraction ϕ for a force density $\alpha(r) = -2\beta(r) = \phi r^2$ and Carman-Kozeny length $\ell_0 = 1$.

Fig.2 as a function of gel fraction. The velocity vanishes for $\phi \rightarrow 0$, because the active forcing is assumed to be associated with the gel fraction and in our simple model is taken to be proportional to ϕ . It also vanishes for $\phi \rightarrow 1$, when the droplet is completely rigid and active forces cannot generate flow. These two limits imply the nonmonotonic dependence of v_g on gel fraction, which is a general feature of our model. In all examples discussed below, we put the viscosity $\eta = 1$ and choose it to be ten times the viscosity of the ambient fluid.

Note that for $\ell \rightarrow \infty$ (*Stokes limit*) and $\phi < 1$ the model must and in fact does reproduce the results for a droplet without interaction with a rigid gel [3]. The limit is not immediately obvious and requires an expansion of $u_0(1/\ell)$ and $u'_0(1/\ell)$ up to order $1/\ell^4$ to see that apparently diverging terms cancel out. The flow field of Stokes equation is an algebraic function of r and hence has no inherent length scale. The crossover from Brinkman flow to Stokes flow is thus

determined by the only available lengthscale, namely the radius of the droplet, which has been set equal to one, defining the unit of length. Hence we expect to see Stokes flow for $\ell \gg 1$. In Fig. 3, we show the flow fields, $v_0(r)$ (a) and $v_1(r)$ (b), for the simple forcing $\alpha(r) = -2\beta(r) = \phi r^2$. The Stokes flow is seen to be a good approximation to the Brinkman flow even for $\ell \gtrsim 1$.

A simple way to introduce a forcing lengthscale is to consider fourth order polynomials of the form,

$$\alpha(r) = \alpha_2 r^2 + \alpha_4 r^4 \quad (22)$$

$$\beta(r) = \beta_2 r^2 + \beta_4 r^4. \quad (23)$$

The parameters $\alpha_i, \beta_i, i = 1, 2$ are restricted by the condition of Eq.(9), which takes on the form $7(\alpha_2 + 2\beta_2) + 5(\alpha_4 + 2\beta_4) = 0$. The resulting inhomogeneous pressure and velocity fields are given by (see Appendix B for details):

$$p^{inh}(r) = \frac{2\alpha_2 - \beta_2}{5}r^3 + \frac{3\alpha_4 - \beta_4}{14}r^5 \quad (24)$$

$$w_0(r) = A_4 r^4 + (A_2 + 28\kappa A_4)r^2 + (10\kappa A_2 + 280\kappa^2 A_4)$$

The constants are given by $A_2 = \frac{-\kappa(\alpha_2 - 3\beta_2)}{5\eta}$ and $A_4 = \frac{-\kappa(\alpha_4 - 5\beta_4)}{14\eta}$. In Fig. 3 we show $v_0(r)$ (c) and $v_1(r)$ (d) for several values of ℓ and a forcing corresponding to Eq.(22) with $\alpha_2 = 10\phi, \alpha_4 = -14\phi, \beta_2 = -5\phi$ and $\beta_4 = 7\phi$. The forcing is maximum for $r \approx 0.6$ and changes sign around $r \approx 0.8$, giving rise to nonmonotonic flow for $r < 1$.

3.3 Dissipated Power

In the stationary state the dissipated energy is balanced by the power input due to the active forces. In addition to the usual viscous energy dissipation $\partial E_\eta / \partial t = \int d^3x \sigma_{i,k} \partial_k v_i$ in both, the inside and outside fluid, we identify an additional energy dissipation due to friction between gel and fluid:

$$\frac{\partial E_\kappa}{\partial t} = \frac{\eta}{\kappa} \int_V d^3x (\mathbf{v} - \mathbf{v}_g)^2. \quad (25)$$

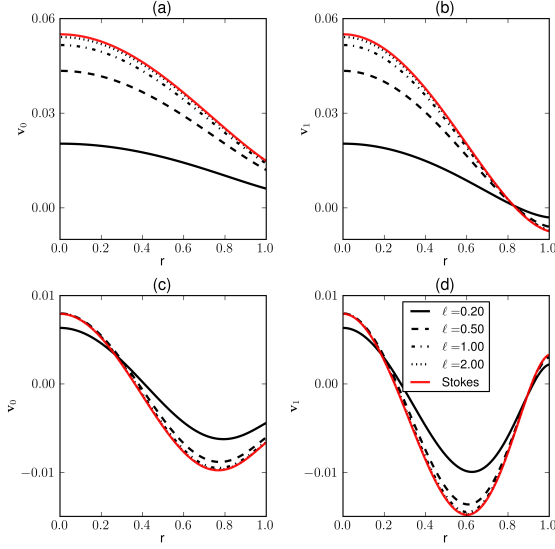


Figure 3: (a) and (b): Radial velocity $v_0(r)$ and tangential velocity $v_1(r)$ for a simple force density with $\alpha(r) = -2\beta(r) = 2\phi r^2$. ((c) and (d)): for a force density corresponding to Eq.(22) with $\alpha_2 = 10\phi$, $\alpha_4 = -14\phi$, $\beta_2 = -5\phi$ and $\beta_4 = 7\phi$. In both cases, $\phi = 1/2$, so that ℓ and the Karman-Cozeny length ℓ_0 coincide. The label "Stokes" refers to $\ell \rightarrow \infty$.

All 3 contributions are compensated by the power input, P_{trans} , due to the active forces

$$P_{act} = \int \mathbf{v} \cdot \mathbf{f}^{act} dV = \int_0^1 [\alpha(r)v_0(r) + 2\beta(r)v_1(r)] r^2 dr. \quad (26)$$

The power input is plotted in the inset of Fig. 4 as a function of gel fraction. Not surprisingly, do we observe the same nonmonotonic dependence as for the flow field.

To quantify the efficiency of the propulsion mechanism we use Lighthill's measure [22, 23],

$$\epsilon = \frac{P_{ext}(\mathbf{v}_g)}{P_{act}}, \quad (27)$$

which compares the dissipated power to the corresponding power, P_{ext} , needed to move a passive droplet by a constant external force, \mathbf{F}_{stall} , with the

same velocity \mathbf{v}_g . Alternatively one can think of \mathbf{F}_{stall} as the force which is necessary to keep an active droplet at rest; we therefore call it stall force. The stall force is related to \mathbf{v}_g via the mobility μ , $\mathbf{F}_{stall} = \mu^{-1}\mathbf{v}_g$, so that $P_{ext}(\mathbf{v}_g) = \mathbf{v}_g \cdot \mathbf{F}_{stall} = \mu^{-1}\mathbf{v}_g^2$. The mobility μ smoothly interpolates between the result for a droplet as $\phi \rightarrow 0$ and the result for a solid particle for $\phi \rightarrow 1$, as is calculated in Appendix C. The efficiency is monotonically decreasing in gel fraction ϕ as shown in Fig. 4.

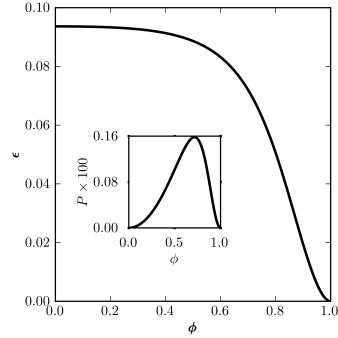


Figure 4: Lighthill efficiency vs. gel fraction for an active force density with $\alpha(r) = -2\beta(r) = \phi r^2$. Inset: Dissipated power

4 Rotational motion

Let us next consider rotational motion of the droplet generated by a chiral force density

$$\mathbf{f}_{rot}^{act}(\mathbf{r}) = \gamma(r)\mathbf{e}_r \times \nabla_s Y_{10} \quad (28)$$

with a single $l = 1, m = 0$ mode. The internal flow field

$$\mathbf{v}(\mathbf{r}) = v_2(r)\mathbf{e}_r \times \nabla_s Y_{10} \quad (29)$$

is divergence free and is calculated from

$$\frac{d^2 v_2}{dr^2} + \frac{2}{r} \frac{dv_2}{dr} - \frac{2}{r^2} v_2 - \frac{1}{\kappa} v_2 = -\frac{\gamma(r)}{\eta} + \frac{\omega_{g0} r}{\kappa}. \quad (30)$$

¹Note that there is a misprint in Eq. (3.10) of reference [3], where $\mu\mathbf{v}_{cm}$ must be replaced by $\mu^{-1}\mathbf{v}_{cm}$.

The differential equations for v_0 and v_2 remain uncoupled, should both active forces \mathbf{f}_{trans}^{act} and \mathbf{f}_{rot}^{act} be present simultaneously.

The solution procedure is completely analogous to the case of linear motion. We split $\mathbf{v} - \boldsymbol{\omega}_g \times \mathbf{r} = (v_2 + \omega_{g0}r)\mathbf{e}_r \times \nabla_s Y_{10} = (v_2^{hom} + w_2(r))\mathbf{e}_r \times \nabla_s Y_{10}$. In this case, the solution of the homogeneous equation is given by $v_2^{hom}(r) = Bu_2(r/\sqrt{\kappa})$ with

$$u_2(x) = x^{-1/2}I_{3/2}(x), \quad (31)$$

and w_2 is a special solution of Eq.(30) with $\omega_{g0} = 0$. The outer solution is given by $v_2^+ = c^+/r^2$ and it is easily checked, that it carries an angular momentum current, which does not vanish at infinity. Therefore c^+ has to be zero for any autonomous swimmer. This implies that the swimming ($l=1$) mode, which causes the rotation of the droplet, leaves no trace in the ambient fluid. The boundary conditions (see Appendix A) thus give us two linear equations to determine B

$$B = - \left(\frac{w_2 - w_2'}{u_2 - u_2'} \right)_{r=1} \quad (32)$$

and $\omega_{g,0}$

$$\omega_{g,0} = \left(\frac{w_2' u_2 - w_2 u_2'}{u_2 - u_2'} \right)_{r=1}. \quad (33)$$

A torque free force distribution cannot be achieved with a single power law, but requires a nonmonotonic force. As for the case of linear motion we can find analytical solutions for all polynomial $\gamma(r)$ given in Appendix B. As a simple illustrating example of a torque free force distribution we choose

$$\gamma(r) = \gamma_0 \phi \left(\frac{r}{7} - \frac{r^3}{5} \right), \quad (34)$$

which leads to

$$v_2(r) = Bu_2(r/\sqrt{\kappa}) + \frac{\gamma_0 \phi \kappa}{\eta} \left[\left(\frac{1}{7} - 2\kappa \right) r - \frac{1}{5} r^3 \right] - \omega_{g,0} r \quad (35)$$

The angular velocity of the droplet is shown in the left part of Fig. 5 as a function of gel fraction. As discussed above, the dependence is nonmonotonic,

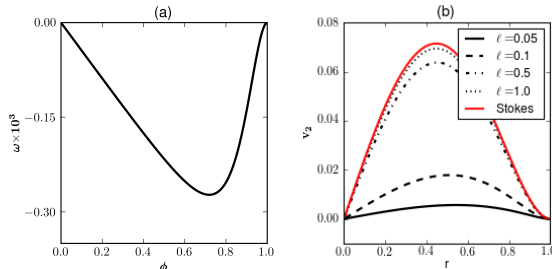


Figure 5: (a): angular velocity versus gel fraction ϕ with $\ell_0 = 1$; (b) $v_2(r)$ versus r for several ℓ and $\phi = 1/2$; for both (a) and (b) the force density is characterised by $\gamma(r) = (5r - 7r^3)2\phi$.

and ω_g vanishes for $\phi = 0$ and $\phi = 1$, so that its overall ϕ -dependence is similar to the linear velocity. The tangential flow field is displayed in the right panel of Fig. 5; it is nonmonotonic as a function of r . Its maximum hardly depends on ℓ and coincides approximately with the corresponding maximum in the forcing density.

5 Darcy Flow versus Brinkman Flow in the limit $\ell \rightarrow 0$

In the limit $\ell \rightarrow 0$ both, the velocities and the viscous stresses vanish in the interior of the droplet. However the rescaled interior flow fields $\hat{\mathbf{v}} = \mathbf{v}/\ell^2$ and the droplet velocities $\hat{v}_{g,0} = v_{g,0}/\ell^2$, $\hat{\omega}_{g,0} = \omega_{g,0}/\ell^2$ remain finite, as will be shown explicitly below. In the following, we will therefore focus on a discussion of these rescaled quantities, which we denote by an additional caret. For $\ell^2 = 0$ the equation for $\hat{\mathbf{v}}$ becomes the Darcy equation

$$(\hat{\mathbf{v}}^D(\mathbf{r}) - \hat{\mathbf{v}}^{gel}) = \frac{1}{\eta} (\mathbf{f}^{act}(\mathbf{r}, \phi) - \nabla p(\mathbf{r})), \quad (36)$$

which is frequently used to study flows in porous media [24]. Therefore let us consider the approximation $\mathbf{v} \approx \ell^2 \hat{\mathbf{v}}^D$ for $\ell \ll 1$ in detail and discuss to what extent properties of an active porous droplet can be obtained from Darcy's equation. The second order spatial derivative of the Brinkman equation for

rescaled flow is multiplied by ℓ^2 . This indicates that the Darcy limit is a singular perturbation problem, and we cannot expect that the leading order term of Brinkman flow for $\ell \rightarrow 0$ coincides with $\hat{\mathbf{v}}^D$. In particular, the Darcy equation, when supplemented by the incompressibility condition, is a system of first order partial differential equations, which cannot fulfil all the boundary conditions of the second order Brinkman equation. Several physical arguments have been put forward to generate a mathematically well-posed problem for systems, which contain an interface between a Darcy medium and a viscous fluid [25].

First we consider the simpler case of rotational motion. To obtain \hat{v}_2^{hom} for $\ell \ll 1$ we use the asymptotic behaviour of the modified Bessel functions, $I_\nu(x) \rightarrow \exp(x)[1 - (4\nu^2 - 1)/8x + O(x^{-2})]/\sqrt{2\pi x}$ for $x \gg 1$. Thus the function $u_2(r)$ defined in Eq.(31) has an essential singularity $u_2(r/\ell) \rightarrow \ell \exp(r/\ell)/(\sqrt{2\pi} r)$ for $\ell \rightarrow 0$, and from Eq.(32) we find that $B \rightarrow \sqrt{2\pi} b \ell^2 \exp(-1/\ell)$. Consequently,

$$\hat{v}_2^{hom}(r) = \frac{Bu_2(r)}{\ell^2} \rightarrow \frac{b\ell}{r} e^{(r-1)/\ell} \quad (37)$$

and the function as well as all its derivatives vanish faster than any power of ℓ in the interior of the droplet, provided $x = r/\ell \gg 1$. At the interface $r = 1$, $\hat{v}_2^{hom}(1) \rightarrow b\ell$, and it contributes to the tractions as $\hat{t}_2^{hom}(1) \rightarrow \eta \hat{v}_2^{hom}(1)/\ell = \eta b$ – even at $\ell = 0$. Thus, the rescaled traction of the homogeneous Brinkman flow does not vanish for $\ell \rightarrow 0$ and contributes to the boundary conditions Eqs.(A.17, A.18), which become $b\ell = \hat{\omega}_{g,0} - \hat{w}_2(1) \rightarrow 0$ and $b - \hat{\omega}_{g,0} - \hat{w}'_2(1) = 0$ for $\ell \rightarrow 0$. For Darcy flow, the homogeneous solution is strictly 0, so that $b = 0$ holds from the outset. Consequently there is no consistent solution for $\hat{\omega}_{g,0}^D$. If we require $\hat{\omega}_{g,0}^D = \hat{\omega}_{g,0}$ the Darcy flow fulfils the boundary condition for the rescaled velocity \hat{v}_2 (see Eq.(A.17)), but there remains a slip in the tangential traction \hat{t}_2 at the interface, i.e. Eq.(A.18) is violated.

In Fig. 6 we show $\hat{v}_2(r)$ and $\hat{t}_2(r)$ for the special forcing $\gamma(r)$ of Eq.(34) in comparison to the flow field, $\hat{v}_2^D(r) = -\hat{\omega}_{g,0}^D r + \gamma(r)/\eta$, of the Darcy equation. Note that we have chosen the value $\hat{\omega}_{g,0}^D = \gamma(1)/\eta$ of the Brinkman flow in the Darcy flow to enable a

comparison. As expected from our discussion, the convergence of the Brinkman flow to the Darcy flow is uniform in r , but the rescaled tractions develop a boundary layer. Thus our discussion has revealed that for small ℓ the Darcy solution is a good approximation to the Brinkman flow in a frame of reference co-rotating with the gel, it also approximates the corresponding viscous traction in the interior outside of a boundary layer at the interface, but it cannot explain the self-propelling property.

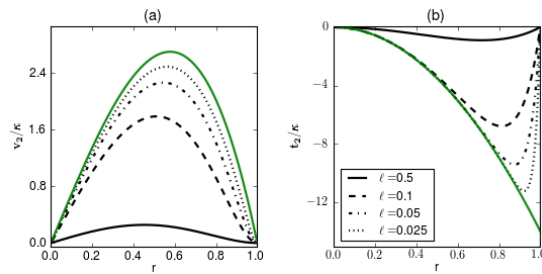


Figure 6: v_2/κ and t_2/κ vs. r for different values of $\ell = \sqrt{\kappa}$ in comparison to the Darcy solution, demonstrating the uniform convergence of the Brinkman flow towards the Darcy flow (a) and the existence of a boundary layer in the tractions (b).

The case of linear motion is similar, but slightly more complicated due to the pressure contribution. As for the rotational motion, we can use the asymptotics of the Bessel function to obtain the homogeneous solution of the Brinkman equation, $v_0^{hom} = Au_0(r/\ell)$, in the limit $\ell \rightarrow 0$. As for the rotational motion $u_0(r/\ell) \rightarrow \ell^2/(\sqrt{2\pi} r^2) \exp(r/\ell)$, has an essential singularity at $\ell = 0$. With $A = \sqrt{2\pi} a \ell^2 \exp(-1/\ell)$, we find in the limit $\ell \rightarrow 0$:

$$\hat{v}_0^{hom}(r) = \frac{Au_0(r)}{\ell^2} \rightarrow \frac{a\ell^2}{r^2} e^{(r-1)/\ell}. \quad (38)$$

Analogous to the case of rotational motion, v_0^{hom} generates a finite rescaled tangential traction $\hat{t}_1^{hom} = \hat{t}_1^{hom}(1)/\ell^2 \rightarrow \eta(v_0^{hom})''/(2\ell^2) \rightarrow \eta a/2$ at the interface in the limit $\ell \rightarrow 0$. The contribution to the radial traction becomes $\hat{t}_0^{hom}(1)/\ell^2 \rightarrow -(p_0 + p^{inh}(1))/\ell^2 + 2\eta \hat{w}'_0(1)$. From the solution for poly-

nomial force densities (see Appendix B) we find that $p_0 + p^{inh}(1) = O(\ell^2)$, and from Eq. (A.13) one reads off that $p_0 \rightarrow \eta(a\ell^2 + w_0(1))$. Thus, even in the limit $\ell \rightarrow 0$ the rescaled pressure on the interface contains a non-vanishing term proportional to a , which results from the homogeneous flow. If we put $a = 0$, as required for the Darcy equation, no consistent solution for $\hat{v}_{g,0} = b^+/\ell^2$ can be obtained from the boundary conditions Eqs.(A.13-A.15).

Let us illustrate this in more detail for the simple force density $\alpha(r) = -2\beta(r) = \alpha\phi r^2$. From Eqs.(20, 21) one sees that $p(r) = p_0 r + (\alpha\phi/2)r^3$ and $\hat{w}_0(r) = -\alpha\phi(r^2 + 10\ell^2)/(2\eta)$. On the other hand, solving the Darcy equation for this particular force density we find $p^D(r) = p_0^D r + (\alpha\phi/2)r^3$ and $\hat{w}_0^D(r) = -\alpha\phi r^2/(2\eta)$. The boundary condition (A.13) determines $p_0 \rightarrow \eta(a\ell^2 + \hat{w}_0(1)) = \eta a\ell^2 - \alpha\phi(1 + 10\ell^2)/2$ and $p_0^D = -\alpha\phi/2$. Hence the difference in pressure $\Delta p(r) = p(r) - p^D(r)$ is solely due to the homogeneous pressure and explicitly given by $\Delta p(r) = \ell^2(\eta a - 5\alpha\phi) + O(\ell^4)$. It dominates the difference between the radial tractions of Brinkman and Darcy flow

$$\hat{t}_0 - \hat{t}_0^D \rightarrow \frac{(p_0^D - p_0)r}{\ell^2} = (\eta a - 5\alpha)r, \quad (39)$$

and is *not* restricted to a boundary layer but a bulk effect. Inserting these asymptotic forms for $\ell \ll 1$ into the boundary conditions Eqs.(A.14, A.15) we get $\hat{v}_{g,0} = \alpha\phi/3\eta + O(\ell^2)$ and $\eta^+ \hat{v}_{g,0} = \eta a - 3\alpha\phi + O(\ell^2)$ which are obviously inconsistent for $a = 0$.

The approach of the rescaled flow fields and tractions towards their limits is shown in Fig. 7 and Fig. 8. To allow for a comparison with Darcy flow, $\hat{v}_0^D(r) = -(\alpha\phi r^2/2 - p_0^D)/\eta + v_{g,0}^D$, we have set $v_{g,0}^D = v_{g,0}$. The radial and tangential flow fields are observed to approach the Darcy solution uniformly in the interior (Fig. 7). On the other hand the rescaled pressure and radial tractions of the Brinkman solution differ from the Darcy solution in all of the interior bulk, as demonstrated in the left part of Fig.8. The difference in tangential tractions is restricted to a boundary layer as for the torsional tractions for the rotational motion.

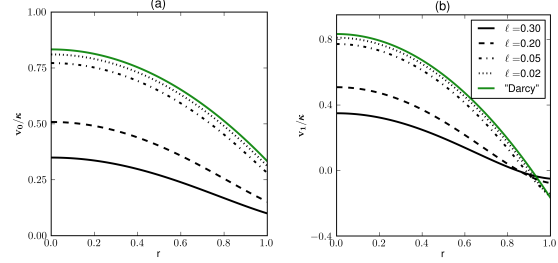


Figure 7: Radial (a) and tangential (b) flow fields, v_0, v_1 , in comparison to the Darcy solution, showing uniform convergence of the flow fields as $\ell \rightarrow 0$.

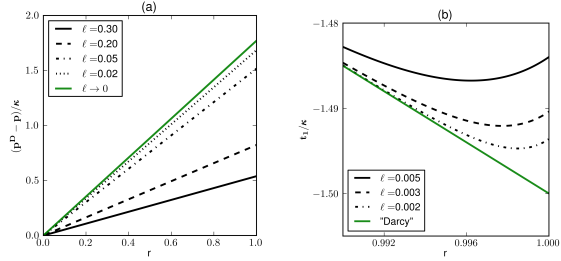


Figure 8: (a) $(p^D - p)/\kappa$ is the asymptotic difference of rescaled radial tractions, shown vs r . This difference is not confined to a boundary layer at the interface. (b) tangential traction t_1 for several values of ℓ in comparison to the Darcy solution, displaying the emergence of a boundary layer for decreasing ℓ .

6 Conclusions and Outlook

We have proposed a biphasic model for an active swimmer, consisting of a gel and a viscous fluid. Building on previous work on porous media, we model the fluid interacting with a rigid gel by Brinkman's equation. The permeability of the gel, κ , defines a characteristic lengthscale $\ell = \sqrt{\kappa}$, which depends on the gel fraction ϕ . It decreases monotonically with gelfraction: If the gel fills the droplet completely, the lengthscale vanishes. In the opposite limit, for very small gel fraction the lengthscale ℓ diverges and we recover Stokes flow.

Activity is modelled by active forces, residing on the gel. We assume their magnitude to be proportional to the gel fraction. The resulting linear and rotational propulsion velocity of the swimmer are non-monotonic functions of the gel fraction ϕ . Both velocities vanish for $\phi \rightarrow 0$, because the strength of the active forces go to zero, and they also vanish as $\phi \rightarrow 1$, because the forces cannot generate internal flow in the space filling rigid gel. Hence there is an optimal gel fraction, giving rise to maximal linear and rotational propulsion. We also discuss energy dissipation, which in addition to viscous dissipation inside and outside of the droplet has an additional contribution from the viscous drag between gel and fluid. Modelling active body forces allows us to introduce another lengthscale which can give rise to nonmonotonic flow as a function of r inside the droplet.

As the gel fraction approaches one, the lengthscale goes to zero and one might naively expect that the flow follows Darcy's equation. However this is not the case, because $\ell \rightarrow 0$ is a singular limit of the Brinkman equation: The solution of the homogeneous equation, $\mathbf{v}^{hom}(r)$, acquires an essential singularity, so that the homogeneous flow and all its derivatives vanish faster than any power of ℓ in the interior of the droplet. For Darcy's equation the boundary conditions cannot be fulfilled and there is no consistent solution for \mathbf{v}_{gel} . Hence the Darcy equation cannot explain self-propulsion.

If we enforce the correct \mathbf{v}_{gel} in the Darcy equation, then the flow fields within the droplet are well approximated by Darcy flow for $\ell \rightarrow 0$. However the pressure in the bulk of the droplet is not accounted for by Darcy's equation and the tangential and torsional tractions are incorrect in a boundary layer, reflecting the incompatibility of Darcy's equation with the boundary conditions.

Even though we have explicitly discussed body forces only, the treatment of surface tractions is straightforward. Similarly, the restriction to $m = 0$ was chosen for simplicity and can easily be lifted. As far as self-propulsion is concerned the expansion in angular momenta can be restricted to $l = 1$, the only mode which contributes to self-propulsion. A correct description of the flow fields inside and outside of the droplet requires inclusion of all l , which is easily

feasible.

Our approach can be extended in several ways. Our model of the gel as a completely rigid porous structure, should be improved. A first step is to consider an elastic gel, a next step could be a viscoelastic medium including dynamics of the gel. So far we have only discussed the simplest forcing. However, the approach is general enough to allow for a more realistic modelling of biological forcing mechanisms, such as an ensemble of motors, moving along a filamentary structure. Work along these lines is in progress.

7 Authors contributions

All the authors were involved in the preparation of the manuscript. All the authors have read and approved the final manuscript.

A Boundary conditions

The interface ∂V of the spherical droplet at $r = 1$ is a free boundary, and the flow field is continuous across ∂V . The velocity components inside the droplet are given by $v_a(r) = v_a^{hom}(r) + v_a^{inh}(r) + v_{g,0}$ (for $a = 0, 1$), $v_0 = Au_0(r/\sqrt{\kappa}) + w_0(r) - (\kappa/\eta)p_0 + v_{g,0}$ and $v_2(r) = Bu_2(r/\sqrt{\kappa}) + w_2(r) - \omega_{g,0}r$. The incompressibility condition determines v_1 in terms of v_0 : $v_1(r) = v_0(r) + rv_0'(r)/2$. Here and in the following the prime denotes the derivative with respect to r . The external flow field is determined by $v_0^+(r) = a^+/r + b^+/r^3$, $v_2 = c^+/r^3$ and the linear velocity $v_{g,0}$ coincides with $v_0^+(r = 1)$.

The viscous tractions $\mathbf{t}^\pm = \pm \boldsymbol{\sigma}^\pm \cdot \mathbf{e}_r$ in a spherical geometry are represented in the from [3]:

$$\mathbf{t} = t_0(r)Y_{10}\mathbf{e}_r + t_1(r)\nabla_s Y_{10} + t_2(r)\mathbf{e}_r \times \nabla_s Y_{10}. \quad (\text{A.1})$$

The flow inside the droplet gives the following contributions

$$t_0^-(r) = -p_0(r) - p^{inh}(r) + 2\eta v_0'(r) \quad (\text{A.2})$$

$$t_1^-(r) = \eta \left(v_1' + (v_0(r) - v_1(r))/r \right) \quad (\text{A.3})$$

$$t_2^-(r) = \eta (v_2' - v_2/r). \quad (\text{A.4})$$

whereas the outside flow and hence the tractions \mathbf{t}^+ are the same as in [3].

Using these quantities, the boundary conditions take on the form of 6 linear equations for the unknowns a^+, b^+, c^+, A, p_0, B . The two equations involving v_2 and t_2 are decoupled from the rest, which takes on the form:

$$0 = Au_0 + w_0 - \frac{\kappa}{\eta} p_0 \quad (\text{A.5})$$

$$-\frac{a^+ + 3b^+}{2} = A \left(u_0 + \frac{u'_0}{2} \right) \quad (\text{A.6})$$

$$+ \left(w_0 + \frac{w'_0}{2} \right) - \frac{\kappa}{\eta} p_0$$

$$-3\eta^+(a^+ + 2b^+) = -p_0 - p^{inh} + 2\eta(Au'_0 + w'_0) \quad (\text{A.7})$$

$$3\eta^+b^+ = \eta(v'_1 - v_1 + v_0). \quad (\text{A.8})$$

The remaining equations become

$$c^+ = Bu_2 + w_2 - \omega_{g,0} \quad (\text{A.9})$$

$$-3\eta^+c^+ = \eta[B(u'_2 - u_2) + w'_2 - w_2] \quad (\text{A.10})$$

Here all functions are taken at $r = 1$ and the prime denotes the derivative with respect to r , for example $u'_0 = du_0/dr = (1/\sqrt{\kappa})(du_0(x)/dx)_{x=1/\sqrt{\kappa}}$.

From the force-free and torque-free condition, we find that $a^+ = 0$ and $c^+ = 0$. The vanishing of c^+ is obvious from the r^{-3} dependence of the outer flow field, which leads to r^{-4} dependence of the viscous stress and thus to a non-vanishing total torque acting on the entire system, in contradiction to the torque-free condition. The vanishing of a^+ can be inferred by adding up two times Eq. (A.8) and Eq.(A.7), which gives

$$-3\eta^+a^+ = t_0^- + 2t_1^- \quad (\text{A.11})$$

On the r.h.s. of this equation we can use

$$\int_{\partial V} \mathbf{t} d^2S = \int_{\partial V} (t_0 Y_{10} \mathbf{e}_r + t_1 \nabla_s Y_{10}) d^2S \quad (\text{A.12})$$

$$= \int_V \nabla \cdot \boldsymbol{\sigma} d^3V = \sqrt{\frac{4\pi}{3}} (t_0 + 2t_1) \mathbf{e}_2.$$

Inserting $\nabla \cdot \boldsymbol{\sigma} = -\mathbf{f}$, one can replace $t_0 + 2t_1$ by $-\int_0^1 (\alpha + 2\beta)r^2 dr$, and thus the r.h.s of Eq.(A.11) becomes the force-free condition Eq. (9).

Using $a^+ = 0$ and subtracting Eq.(A.5) from Eq. (A.6) leaves us with three linearly independent equations, which can be written in the form

$$p_0 = \frac{\eta}{\kappa} (Au_0 + w_0) \quad (\text{A.13})$$

$$b^+ = v_{g0} = -\frac{1}{3}(u'_0 A + w'_0) \quad (\text{A.14})$$

$$6\eta^+b^+ + 2\eta u'_0 A - p_0 = -2\eta w'_0 + p^{inh} \quad (\text{A.15})$$

Solving the last two equations for A , yields the result given in Eq. 19 in the main text. Note that with Eq.(A.5) the radial velocity field $v_0(r)$ becomes

$$v_0(r) = Au_0(r) + w_0(r) + v_{g0} - \frac{\kappa p_0}{\eta} \quad (\text{A.16})$$

$$= A(u_0(r) - u_0(1))$$

$$+ (w_0(r) - w_0(1)) + v_{g0}.$$

In this form it is given in the main text in Eq.(18).

For rotational motion Eqs. (A.9- A.10) simplify for $c^+ = 0$:

$$(Bu_2 - \omega_{g,0} + w_2)_{r=1} = 0 \quad (\text{A.17})$$

$$(Bu'_2 - \omega_{g,0} + w'_2)_{r=1} = 0. \quad (\text{A.18})$$

with the explicit solution given in Eqs. (32,33).

B Flow fields from polynomial force densities

Here we discuss special solutions of Eqs. (20, 17) and Eq.(30), for force densities with polynomial $\alpha(r), \beta(r), \gamma(r)$, like $\alpha(r) = \alpha_0 + \alpha_1 r + \alpha_2 r^2 + \dots$.

The pressure equation (20) has polynomial solutions, provided we put $\alpha_0 = \beta_0$. (For $\alpha_0 \neq \beta_0$, terms $\propto r \ln r$ will also occur.) For n th order monomials, $\alpha_n r^n$ and $\beta_n r^n$, a particular solution, regular at $r = 0$, is given by

$$p^{inh}(r) = \frac{(n+2)\alpha_n - 2\beta_n}{n(n+3)} r^{n+1} = p_n^{inh} r^{n+1}. \quad (\text{B.1})$$

Note that for $n = 2$ and $n = 4$ this produces Eq.(24).

All inhomogeneities in Eq.(17) are thus polynomials $\sum_{n=0} D_n r^n$ with $D_n = (p_n^{inh}(n+1) - \alpha_n)/\eta$.

For example, $D_2 = (\alpha_2 - 3\beta_2)/5\eta$ and $D_4 = (\alpha_4 - 5\beta_4)/14\eta$.

For every monomial of even order, $D_{2m}r^{2m}$, it is easy to find a solution from the ansatz

$$w_0 = A_{2m}r^{2m} + A_{2m-2}r^{2m-2} + \dots + A_2r^2 - A_0.$$

It leads to $A_{2k-2} = 2k(2k+3)\kappa A_{2k}$ for $k = 1, 2, \dots, m$, which allows to determine the A_{2k} starting from $A_{2m} = -\kappa D_{2m}$.

So, for example, for force densities $\propto r^2$, corresponding to $m = 1$, this leads to

$$w_0^{m=1} = A_2(r^2 + 10\kappa), \quad (\text{B.2})$$

with $A_2 = -\kappa D_2$, and for $m = 2$ we get

$$w_0^{m=2} = A_4(r^4 + 28\kappa r^2 + 280\kappa^2). \quad (\text{B.3})$$

In the main text, we considered both r^2 and r^4 terms to be present, so that

$$\begin{aligned} w_0 &= w_{04}r^4 + w_{02}r^2 + w_{00} \\ &= A_4r^4 + (A_2 + 28\kappa A_4)r^2 + (10\kappa A_2 + 280\kappa^2 A_4) \end{aligned} \quad (\text{B.4})$$

For odd order monomials $D_{2m+1}r^{2m+1}$ a polynomial ansatz for w_0 is not sufficient. Extending the ansatz by terms $A_{-1}r^{-1}$ and $A_{-3}r^{-3}$ does lead to solutions, but they are not regular at $r = 0$. To construct solutions, which stay regular in the droplet's interior, one has to add a homogeneous solution, which compensates the singular terms. A regular solution takes on the form

$$\begin{aligned} w_0 &= C(r/\sqrt{\kappa})^{-3/2} K_{3/2}(r/\sqrt{\kappa}) + (-8r^{-2} \\ &+ 4r^{-1} + r)A_1 + \dots - \kappa D_{2m+1}r^{2m+1}. \end{aligned} \quad (\text{B.5})$$

and the coefficients A_{2k+1} can be determined in analogy to the case of even order inhomogeneities.

Starting from Eq. (30) and polynomials $\gamma(r)$ we can proceed analogously to construct w_2 . Odd order monomials $\gamma_{2n+1}r^{2n+1}$ lead to polynomial solutions $w_2 = B_{2n+1}r^{2n+1} + B_{2n-1}r^{2n-1} + \dots + B_1r$ with $B_{2n+1} = \kappa\gamma_{2n+1}/\eta$ and $B_{2k-1} = \kappa[(2k+1)(2k+2) - 2]B_{2k+1}$. For even order monomials, the Polynomial Ansatz has to be extended by terms $B_0 + B_{-2}r^{-2}$ and a regular solution has to be constructed by adding a homogeneous solution $F(r/\sqrt{\kappa})^{-1/2} K_{3/2}(r/\sqrt{\kappa})$.

C Stall force and mobility

To move a passive droplet with velocity v_g in z -direction, one applies a constant force density $\mathbf{f}_{stall} = f\mathbf{e}_z = -\nabla U$, which gives rise to a total force $F = 4\pi f/3$.

The inhomogeneity in Eq. 1 is then given by $\nabla p(\mathbf{r}) - \mathbf{f}_{stall} = \nabla \tilde{p}$, so that the stall force can be absorbed into a modified pressure $\tilde{p} = p - U$. The latter fulfils Laplace equation, whose solution is given by $\tilde{p}(\mathbf{r}) = \tilde{p}_0 r Y_{10}(\theta, \varphi)$ with $\tilde{p}_0 = (p_0 - \sqrt{4\pi/3}f)$. The only inhomogeneity in Eq. 17 is \tilde{p}_0 , so that $w_0 = 0$. The set of Eqs. A.5 to A.8 then reads

$$0 = Au_0 - \frac{\kappa}{\eta} \tilde{p}_0 \quad (\text{C.1})$$

$$-\frac{a^+ + 3b^+}{2} = A \left(u_0 + \frac{u'_0}{2} \right) - \frac{\kappa}{\eta} \tilde{p}_0 \quad (\text{C.2})$$

$$-3\eta^+(a^+ + 2b^+) = -p_0 + 2\eta Au'_0 \quad (\text{C.3})$$

$$3\eta^+ b^+ = A\eta(u'_0 + u''_0/2). \quad (\text{C.4})$$

and has to be solved for the four unknowns A, p_0, a^+, b^+ . Due to the presence of a force, there is a Stokeslet with $a^+ = \sqrt{4\pi/3}f/(3\eta^+)$. The center of mass velocity is given by $v_g = \sqrt{3/(4\pi)}(a^+ + b^+) = \mu F$ with the mobility

$$\mu = \frac{1}{4\pi\eta^+} \left(1 + \frac{\eta(u_0/\kappa - 2u'_0)/3}{2u'_0(\eta - \eta^+) - \eta u_0/\kappa} \right). \quad (\text{C.5})$$

In the Stokes limit $\kappa \rightarrow \infty$ and $u_0/(\kappa u'_0) \rightarrow 5$. This reproduces the well-known mobility $\mu = (\lambda + 1)/[2\pi\eta^+(3\lambda + 2)]$ of a fluid droplet with viscosity contrast $\lambda = \eta/\eta^+$. In the Darcy limit the terms proportional to u'_0 can be neglected and one recovers the mobility of a solid particle.

References

- [1] Lauga E and Powers T 2009 *Rep. Prog. Phys.* **72** 096601
- [2] Goldstein R E and van de Meent J W 2015 *Interface focus* **5** 20150030

- [3] Kree R, Burada P and Zippelius A 2017 *J. Fluid Mech.* **821** 595–623
- [4] Alt W and Dembo M 1999 *Math. Biosciences* **156** 207–228
- [5] Spitzer J and Poolman B 2013 *FEBS Letters* **587** 2094–2098
- [6] Moeendarbary E, Valon L, Fritzsche M, Harris A, Moulding D, Thrasher A, Stride E, Mahadevan L and Charras G T 2013 *Nature Mat.* **12** 253–261
- [7] Callan-Jones A C and Jülicher F 2011 *New J. Phys.* **13** 093027
- [8] Köhler S, Schaller V and Bausch A 2011 *Nature Mat.* **10** 462468
- [9] Keber F C, Loiseau E, Sanchez T, DeCamp S J, Giomi L, Bowick M J, Marchetti M C, Dogic Z and Bausch A R 2014 *Science* **345** 1135–1139
- [10] Weiss M, Frohnmayer J, Benk L, Haller B, Heitkamp J J T, Börsch M, Lira R, Dimova R, Lipowsky R, Bodenschatz E, Baret J, Vidakovic-Koch T, Sundmacher K, Platzman I and Spatz J 2017 *Nature Mat.* **17** 89–96
- [11] Zwicker D, Seyboldt R, Weber C A, Hyman A A and Jülicher F 2014 *Nature Phys.* **13** 408–413
- [12] Zwicker D, Hyman A and Jülicher F 2015 *Phys. Rev. E* **92** 012317
- [13] Durlofsky L and Brady J 1987 *Phys. Fluids* **30** 3329
- [14] Rubinstein J and Torquato S 1989 *J. Fluid Mech.* **206** 25–46
- [15] Tamayol A and Bahrami M 2011 *Phys. Rev. E* **83** 046314–1–9
- [16] Carman P 1956 *Flow of gases through porous media* (London: Butterworths)
- [17] Ochoa-Tapia J and Whitaker S 1995 *Int. J. Heat Mass Transfer* **38** 2635–2646
- [18] Jäger W, Mikelić A and Neuss N 2001 *IAM J. Sci. Comput.* **22** 2006–2028
- [19] Minale M 2014 *Phys. Fluids* **26** 123101
- [20] Minale M 2014 *Phys. Fluids* **26** 123102
- [21] Abramowitz M and Stegun I 1965 *Handbook of Mathematical Functions* (Dover)
- [22] Lighthill M 1952 *Comm. Pure Appl. Math.* **9** 109
- [23] Shapere A and Wilczek F 1989 *J. Fluid Mech.* **198** 587–599
- [24] Vafai K (ed) 2005 *Handbook of Porous Media* (Taylor and Francis)
- [25] Erhardt M 2012 *Progress in Computational Physics (PiCP): Coupled Fluid Flow in Energy, Biology and Environmental Research* vol 2 (Ben-tham) chap 1, pp 3–12